TI SKIN

QUADERNO TECNICO GENERALE – VOLUME ALLEGATI

La documentazione integrale a supporto del Quaderno Tecnico (TISKIN-14): i paper dei progetti di ricerca universitari, l'estratto completo delle simulazioni IDA ICE per il CNR di Pisa, i test di laboratorio e le tavole tecniche, riprodotti dalle pagine originali.

BY PURE ORGANICA CORP.

CON SYNDEGO ITALIA S.R.L.

www.pureorganica.us · info@pureorganica.us · Syndego Italia S.r.l. — www.ti-skin.it

v1.1 — 12 settembre 2026

INDICE DEGLI ALLEGATI

Documenti integrali riprodotti dalle pagine originali del Quaderno Tecnico rev. 01

Nota. Le pagine di questo volume riproducono i documenti originali (paper scientifici, tavole di simulazione, test di laboratorio) così come pubblicati dagli autori e dagli enti citati; l'impaginazione è stata adattata al formato della serie documentale Pure Organica. Questo volume accompagna il Quaderno Tecnico Generale (TISKIN-14) e non lo sostituisce. I rapporti di prova e i certificati ufficiali (resistenza al fuoco USA/Europa, prove termiche) sono documenti dei laboratori emittenti: sono disponibili su richiesta a info@pureorganica.us.

Le fonti, per esteso

Chi vuole verificare trova qui i documenti completi: due paper universitari internazionali, quindici tavole di simulazione dinamica e i test di laboratorio del sistema TI-SKIN.

ALLEGATO A

Progetto di ricerca — Conservazione dell'olio EVO

Abstract

The quality of Extra Virgin Olive Oil (EVOO) is strongly correlated to storage temperature, in fact the storage conditions (packaging material, oxygen, temperature, and light) alters not only the fatty acid alkyl esters (FAEE) of the olive oil but also other quality parameters such as peroxide, making the oil incompatible to the high quality EVOO. During storage of EVOO the polyphenols tend to decrease and compromise the dietetic and nutritional qualities and taste and produce harmful substances. The storage temperature, more than 24°C, influences quite a lot FAEE especially for long term conservation. High storage temperature leads to degradation of oil quality in the long term while low temperature develops rancidity quickly, reducing the consumer's demand. Low storage temperature also affects the EVOO quality but in a lesser way than high storage temperature. The present study proposes the use of a control temperature system based on the application of Phase Change Materials (PCM) on the buildings envelope. A specific case study was considered to evaluate the effect on use of PCM. The building analysed was an olive mill building situated in Scido a small town in the province of Reggio Calabria located in southern Italy. The intervention on the EVOO storage room to improve the energy savings for temperature control was based on the insulation of the partitions and the installation of a false ceiling to limit the air volume, with a two layer panel sandwich, one of PCM and the other of a rigid polyurethane foam with a 4 cm thick metal cladding. a thermal analysis simulation, by means of DesignBuilder software, was conducted. To calculate the electric energy spent in a year to control air temperature in a range of 8-22°C. The results were of 3590. 67 kWh/year for existing building e 2539.52 kWh/year for building with PCM, an energy save of about 30%. A temperature decrease of about 3 °C was measured inside the storage room without a cooling system during the hottest year period but the most important result was a thermal indoor air stabilization in the storage room. This condition avoids a thermal fluctuation to the EVOO and it is the best storage condition.

Keywords: Energy analysis, Extra Virgin Olive Oil, Food building, PCM, Polyphenols.

Allegato A — pagina 11 del documento originale

1 Introduction

Conservation of food production is an important phase because the most important chemical, physical and biological changes take place during this phase (Barbaresi et al., 2015) (Barbaresi et al., 2014), such as some quality parameters of extra virgin olive oil (acidity, peroxide value and UV absorbance) that could vary depending on the time and storage method, leading to undesirable olive oil.

The quality of Extra Virgin Olive Oil (EVOO) is strongly correlated to the fatty acid alkyl esters (FAEE) content. In fact researches which have been carried out have emphasized the relationship between FAEE in olive oil and its sensory classification and also the defects due to olive fermentation. The FAEE determines the organoleptic profile of an EVOO which plays a relevant role in olive oil classification and it is included among the quality parameters (Gómez-Coca et al., 2016). Nevertheless it has been demonstrated how the content of the FAAE at a high concentration, highlights the fact that olive fruits with fermentative alterations and high maturity index had been used for oil extraction. The storage temperature, more than 24°C, influences quite a lot FAEE especially for long term conservation. An incorrect storage temperature interval alters not only the FAEE of the olive oil but also other quality parameters such as peroxide, making the oil incompatible to the high quality EVOO.

The European Commission Regulation of 2016 established that the legal value limit of FAEE content for EVOO is 30 mg/kg.

Allegato A — pagina 12 del documento originale

The concentrated FAEE are not static and under wrong storage conditions they could go over the maximum limit allowed to classify oil as extra virgin, therefore not ranking the highest category. During storage of EVOO the polyphenols tend to decrease and compromise the dietetic and nutritional qualities (Ayton et al., 2012) and taste and produce harmful substances (Lo Curto et al., 2001). Low storage temperature also affects the EVOO quality but in a lesser way than high storage temperature. Researchers noticed that storage temperature below 4°C lasting 15 days causes a decrease of about 50% of the total polyphenols in respect to freshly made EVOO (Piscopo and Poiana, 2012). Storage temperature significantly affects the sensory profile of olive oils. High storage temperature leads to degradation of positive oil attributes in the long term, while low temperature develops rancidity quickly and reducing the consumer's acceptance and therefore the shelf life of EVOO (Ayton et al., 2012).

The best EVOO storage range temperature is very difficult to define, because a lot of parameters influence the optimal temperature interval. Olive cultivar, maturity index of the olive fruits, storage tank type, ambient lighting and time of storage, are only some parameters could affect the best storage temperature. For example the best range of temperature for a typical Calabrian EVOO, made with monovarietal Carolea olives, stored in stainless steel tanks and held in a dark environment with an average storage time of 12 months, is between 8°C and 22°C. (Piscopo and Poiana, 2012)

Allegato A — pagina 13 del documento originale

Usually, the conservation stage consumes more energy than other stages, because the energy spent for product units is related to the time of conservation which is long and often more than one year. For these reasons thermal control of the storage EVOO environment is very important and the use of passive solutions could improve energy savings of the production.

Spain ($1{,}271\cdot10^3$ t) and Italy ($429\cdot10^3$ t) are the main producers of Olive oil in Europe and Italy is the major consumer of olive oil ($560\cdot10^3$ t) (Zolichová, 2017).

Apulia in Italy is the first production region, with 33% of an olive grove surface area, followed by Calabria, with 17% (184,000 ha), of which about 1550 ha are table olive groves and about 183 ha are oil olive groves, producing 140,000 tons of olive oil annually (Stillitano et al., 2017). In Calabria Olive trees are the most cultivated and the most important chain supply, which contribute to local rural economy (Valenti et al., 2017). The greatest surface areas are the provinces of Cosenza and Reggio Calabria (Luca et al., 2018). In particular in the province of Reggio Calabria there is the highest number of olive mills (304) and the highest quantity of olive oil production (26,555 t) (ISMEA, 2018).

The climate in Reggio Calabria is typically Mediterranean, with a mild temperature in winter (T> 0°C) and warm summers (T max > 30°C) , with a strong daytime and night time change of temperature. The environmental indoor temperature of the EVOO mill storage area in summer is often higher than 35°C (Barreca and Praticò, 2018).

Allegato A — pagina 14 del documento originale

The present study proposes the use of a control temperature system based on the application of Phase Change Materials (PCM) on the buildings envelope of an olive mill located in a small town of Reggio Calabria province. This solution avoids a thermal fluctuation to the EVOO and it is the best storage condition, in fact the quality of EVOO depends strongly on the storage temperature.

2 Materials and Methods

A good design of the envelope of a building generally gives an efficient thermal control. In fact the right thermal design of a building should consider the value of a thermal insulation and the thermal capacity of the external partitions (Barreca and Fichera, 2013). The thermal insulation of the walls is very important in cold temperatures whereas the thermal mass of the walls is important in warm temperatures because the material will accumulate excess of heat during the day and will return it in the air when temperature drops during the night. The heat accumulated depends on the mass and on the specific heat of the materials of the wall. Old buildings were build heavy walls endowed with high thermal mass, the modern buildings' walls are lighter with more empty spaces to increase the thermal insulation but this solution decrease the thermal inertia.

The PCM is a heat storage that absorbs the incoming heat flux and removes it from the environment through a melting process, when the temperature decreases, the PCM solidifies and returns the heat to the environment (Caprara and Stoppiello, 2012). The advantage of using the PCM in the building envelope allows:

- to limit the indoor environment heat input and to store it until the indoor temperature decreases
- to maintain a constant indoor air temperature during the melting process

The PCM has two stages called "load" and "unload", in theory these stages could carry on until infinity, but in fact the PCM has a limited number of stages.

Allegato A — pagina 15 del documento originale

The PCM could improve the thermal walls performance because it exchanges heat with the external environment, it absorbs heat when it melts and when it solidifies it releases heat to the environment.

The change phase of the material is with constant temperature and this characteristic is important for insulation material because it allows stabilization of the environmental indoor temperature. Moreover the heat accumulated [1] is due to the exchange of sensible heat when the material is itself in a solid o liquid state:

$$Q = m \int_{T_i}^{T_m} c_{p_s} \, dT + m \, \Delta H_m + \mathrm{m} \int_{T_m}^{T_f} cp_l dT \quad [1]$$

Where:

Q is the heat accumulated (J)
m is the mass of the material which change its phase (g)
ΔH_m is the phase change enthalpy variation of the material ($J \cdot g^{-1}$)
$T_i - T_m$ is the range of temperature of solid material (°C)
$T_m - T_f$ is the range of temperature of liquid material (°C)
c_{p_s} is the specific heat of the solid material ($J \cdot g^{-1} \cdot °C^{-1}$)
cp_l is the specific heat of the liquid material ($J \cdot g^{-1} \cdot °C^{-1}$)

Allegato A — pagina 16 del documento originale

The design process is quite complexed because it has to be carried out by a dynamic thermal model which has to take into consideration the external heat flux and the behaviour of the PCM at different temperatures. Another essential point is to know the correct latent heat curve. In fact the latent heat curve is often not well defined for all PCMs, because a complex procedure needs a differential scanning calorimeter (Osterman et al., 2012).

The base material of the PCM could be organic (hydrated salts) o inorganic (paraffins), research has recently been looking for more new natural substances for the safety of the environment and for occupants of buildings [10]. It is very important to obtain the right environmental temperature by carrying out a correct design of the PCM system, choosing the right type of material and the best melting temperature but at the same time building the PCM system in the right way.

If Phase Change Material (PCM) is used as insulation material of external walls and its temperature is around melting temperature, its behaviour is like that of a total insulation material because the temperature of its mass remains constant until the received thermal energy melts the mass totally (Buonomano et al., 2016). PCM stores not only the latent heat but also a part of sensible heat which changes the temperature of the PCM (Castell et al., 2009).

Allegato A — pagina 17 del documento originale

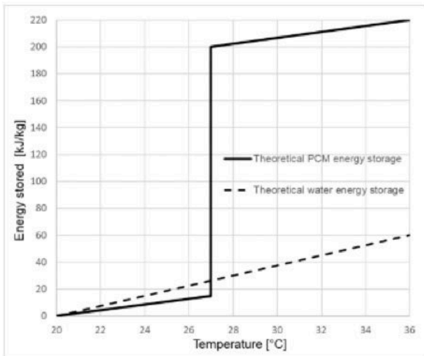

Figure 1. Graph of energy stored and temperature for a PCM

Figure 1 illustrates the energy stored by the PCM. Sensible heat is absorbed in the solid material with temperature that rises from 20 °C to 27 °C (slope of the line is correlated to specific heat of the material), at 27 °C the temperature starts the melting process and the heat absorbed is totally used to melt the material (the temperature in the material remains constant) , when the melting process is completed the heat rises the temperature of the liquid outcome(sensible heat). At the end of the process the energy stored in PCM is the sum of both sensible and latent heat. When external heat flux ends (for example at night) the PCM releases the heat stored before and its temperature decreases until solidification starts therefore bringing the PCM to its initial conditions.

Allegato A — pagina 18 del documento originale

2.1 The EVOO storage room

The building analysed was an olive mill building situated in Scido a small town in the province of Reggio Calabria in southern Italy (coords: 38°15’36.1”N; 15°56’28.6”E). The buildings has 14 x 35 m rectangular plan (fig. 2), the oil storage room has a surface of 130m^2 and the working area has a surface of 450 m^2, the vertical building structures are with reinforced concrete and the roof structures are of steel. The external walls are in hollow brick, the covered of the pitched roof is with insulated metal panels, the internal eave

height is 7 m. The windows of the building are located on each of the two longer sides of the main unit, but they are not located in the storage olive oil area. The internal environment is naturally ventilated and has neither air-conditioning nor ventilation systems. In particular the olive oil storage room has a dimensions of 7.70 m x 17.00 m and it is located north of the building. In the storage olive oil area, there are twelve stainless steel tanks, 6 of 4 m^3 and 6 of 5 m^3, the oil is produced by means of a three-phase system for olive oil extraction from olives cultivar of Carolea and Sinopolese.

Allegato A — pagina 19 del documento originale

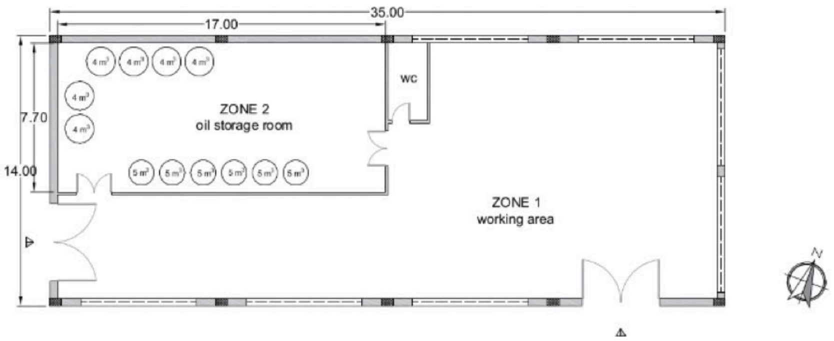

Figure 2 –Plan of the olive mill

Allegato A — pagina 20 del documento originale

2.2 Energy software

The numerical analysis of the PCM needs an advanced software of thermal dynamic analysis which considers the behaviour of the heat capacity of the envelope exposed at a variable external thermal load.. In this case study a Design Builder version 5.4 software was used and the thermal analysis was carried out considering the closest World Meteorological Organization (WMO) weather station n. 164200 located about 35 km West from the olive mill under study (38° 12' N ; 15° 33' E) (fig. 3). The core of this software is EnergyPlus™ 8.6 which is a simulation Software for numerical analysis. EnergyPlus™ 8.6 is a popular program in literature released by the U.S. Department of Energy. The software allows the building division into thermal zones, each zone is defined as a portion of space composed by an air volume at uniform temperature and by its boundary surface the thermal model is built by the pre-processor of DesignBuilder. It is important for this aim, to define the thermal characteristics of the building component materials, in fact the precision of results depend strongly on the accuracy of the material parameter values such as conductivity, specific heat, vapour resistance and thermal and solar absorptance. It is important to define the correct function temperature- enthalpy for the Phase Change Material which will be adopted into the thermal model. The function must cover the entire range temperature that will be used in the numerical simulation and the function temperature-enthalpy should be provided by the PCM producer.

Allegato A — pagina 21 del documento originale

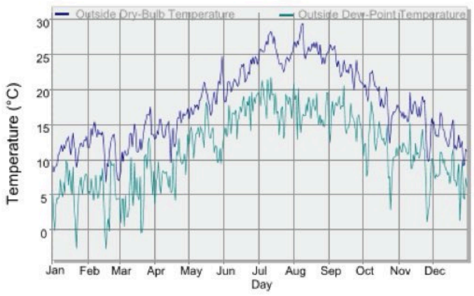

Figure 3 – Site average daily temperature of weather station of the WMO

Allegato A — pagina 22 del documento originale

2.3 Choice of PCM

The intervention on the EVOO storage room to improve the energy savings for temperature control was based on the insulation of the partitions and the installation of a false ceiling to limit the air volume, with a two layer panel sandwich, one of PCM and the other of a rigid polyurethane foam with a 4 cm thick metal cladding. To obtain the PCM layer, about 1 cm thick boards were used which were composed by two sheets of aluminium that enclosed the phase change material made of salt hydrate and which was produced with different melting temperature, varying from 19°C to 29 °C. A simplified energy analysis was conducted, by means of PCM express software, to choose the optimal melting temperature of the phase change material to maintain an air temperature around 22°C during the year. The PCM express software is a free software based on a finite difference mathematical model and on enthalpy method to simulate the PCM behaviour. PCM express was created in connection with the research project "Development of a user-friendly planning and simulation programme in the combined project 'Active PCM storage systems for Building PCM Active' ", that ran in collaboration with the Fraunhofer Institute for Solar Energy Systems ISE in Freiburg and partners from industry (Zöller A., Jung M., Schmidt M., Brenner T., Gatzka B., Schossig P., 2008). The best solution, highlighted by means of the energy analysis, was the panel sandwich with a layer of PCM at 25°C melting temperature, this solution allows a yearly energy savings estimated of about 1000 kWh/year (fig. 4).

Allegato A — pagina 23 del documento originale

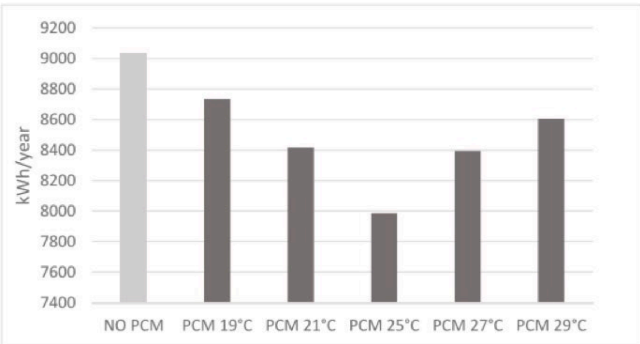

Figure 4 – comparison of PCM from different yearly energy consumption

Allegato A — pagina 24 del documento originale

2.4 Thermal analysis

Thermal analysis requires local weather data in order to model the outdoor weather conditions, that are variable during the seasons. The accuracy of the analysis is correlated to the weather data precision. In this paper the thermal analysis was carried out considering the closest World Meteorological Organization (WMO) weather station n. 164200 located about 35 km West from the olive mill under study (38° 12' N ; 15° 33' E), the weather file is part of the Italian Climate Data Set elaborated by Gianni de Giorgio with a yearly data from 1951 until 1970. The file contains the average hourly statistics for a year of dry and dew bulb temperatures, the relative humidity, the monthly statistics for wind direction and speed and for the global horizontal and normal solar radiation. The weather file was corrected and calibrated by means of a weather data (temperature and humidity) surveyed by a specific station located 50 m from the modelled building. The calibration procedure was carried out to consider the local micro-climate conditions influenced by the orography of the site, in particular different range temperature between day and night. A specific weather file to analyze the building in this manner has been created. The indoor environment of EVOO storage room was conditioned by means of an electric HVAC system. In particular for the EVOO storage a thermal analysis was carried out to evaluate the energy spent to maintain the indoor air temperature around the correct range (8-22 °C). Two different energy models were created: model A, storage room walls without PCM; model B, storage room walls insulated by sandwich panel with PCM (fig. 5) (tab. 1) . A special attention was paid on modelling accurately the olive oil tanks, in fact the scientific literature shows that a big quantity of liquid stored can remarkably affect the thermal inertia of the building (Benni et al., 2013).

Allegato A — pagina 25 del documento originale

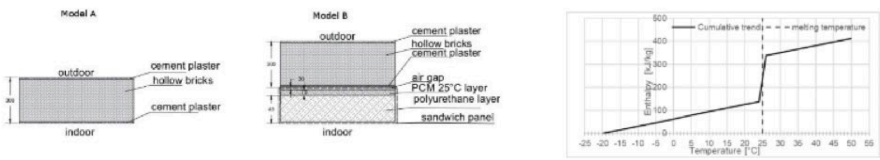

Figure 5 – storage room walls - model A and model B and enthalpy curve of PCM 25°C

Tab. 1 – Thermal characteristics of wall layers for model A and model B

Wall layer	Model A				Model B			
	Thickness [m]	Heat capacity [J/kgK]	Thermal conductivity [W/mK]	Density [kg/m^3]	Thickness [m]	Heat capacity [J/kgK]	Thermal conductivity [W/mK]	Density [kg/m^3]
Cement plaster	0.02	840	0.720	1760	0.02	840	0.720	1760
Hollow brick	0.30	840	0.300	1000	0.30	840	0.300	1000
Cement plaster	0.02	840	0.720	1760	0.02	840	0.720	1760
Air gap					0.03		0.026	
PCM 25°C					0.007	3140	0.810	570
Polyurethane					0.04	1470	0.028	30

Allegato A — pagina 26 del documento originale

The tanks were modelled as solids whose size corresponds to their real volume, the inertia of steel tanks is negligible because they have thin walls, for this reason in the model were considered only the thermal characteristics of the olive oil (Specific Heat =1840 kJ/m^3; Thermal Conductivity at 20°C = 0.17 W/mK) (Turgut et al., 2009). The building's model was divided in two thermal zone, zone 1 the process area of the EVOO, zone 2 the storage room. A thermal analysis simulation, by mean the software DesignBuilder 5.4, was carried out. to calculate a HVAC system's yearly electric energy consumption for controlling air temperature in zone 2 (temperature range of 8-22°C) by a HVAC system (Barreca et al., 2017).

The results were of 3,590.67 kWh/year for model A e 2,539.52 kWh/year for model B, with a save of about 30% of energy .

27

Allegato A — pagina 27 del documento originale

3 Results and discussions

The retrofitting intervention of the buildings was conducted in January 2018 and ended in the same month. The panel sandwich was built in two phases; phase one an PCM 25°C layer (brand Infinite R™ manufactured by INSOLCORP) was applied to the panel sandwich by means of steel structures fixed between the roof and the floor. In phase two a polyurethane layer was installed (Fig. 6 a). The false ceiling was built by fixing the polyurethane layer to the roof truss and the Infinite R-25™ PCM 25°C board was spread out on it, (fig. 6 b) .

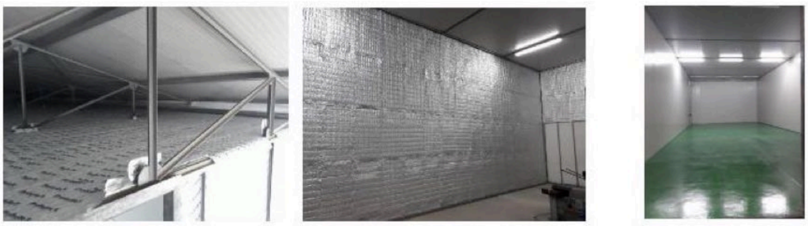

a) b) c)

Figure 6 – PCM sandwich installation phases

28

Allegato A — pagina 28 del documento originale

After the intervention of the storage room (fig. 6c) a thermal survey was conducted to evaluate the thermal performance of the PCM panels. The air temperature of EVOO storage room was monitored from 2 August until 13 September 2018 to intercept the average hottest days in a year. The survey of the temperature was carried out by means of two air temperature sensors, with a resolution of 0.01 °C and a uncertainty of 0.10 °C linked to a data logger, one was installed in the storage room and the other was put next to it. The survey allowed to assess the performance of the adopted solution (Barreca and Tirella, 2017). The comparison between the two temperature sensors highlighted, during the hottest year period, a temperature decrease inside the storage room of about 2.5 °C without a cooling system (fig. 7).

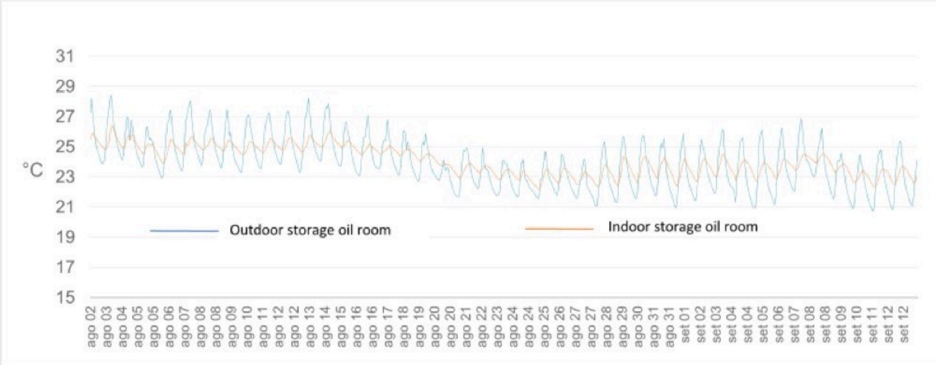

Figure 7 – surveyed measured temperature

The decrease of the indoor air temperature was observed during the hottest year season period, this event demonstrated the good performance of the solution adopted. PCM blocks the input flux heat inside the storage room. When the temperature of the PCM board surface increases more than 24-25° C, the material melts and the changing phase absorbs the exceeded heat flux preventing the indoor air temperature to increase. When the outside air temperature decreases, the phase change material solidifies and the heat outdoor releases the accumulated heat. It is important to note that the best performance of the material is around the melting temperature, in fact if the difference of the PCM work temperature is more than the melting temperature, its behaviour is close to that of a neutral thermal behavior. Instead the second layer of the sandwich panel in polyurethane foam is a thermal resistance for all temperatures and it limits the heat dispersion in a particular way when the external temperature is low (Porto et al., 2017). The most important result was a thermal indoor air stabilization in the storage room. This condition avoids a thermal fluctuation to the EVOO and it is the best storage condition. The quality of EVOO depends strongly on each stage of the production process and also on the environmental condition (Pascale et al., 2018)(Altieri et al., 2015). Many studies carried out showed the alteration of the fatty acid composition and the antioxidant activity during the storage stage. Nowadays it is well known that storage environmental conditions (light, temperature, smell, vibrations) as well as the packing materials (clear PET, can, glass, AISI steel tank) influences the quality of EVOO. In particular there is a strong correlation between temperature and storage time (Escudero et al., 2016) and a more evident effect of a variable storage temperature on the EVOO quality (Li and Wang, 2018). This study is a first stage approach toward the problem solution and the next stage will be the assessment of the qualitative response on oils stored inside the EVOO storage room.

4 Conclusions

The case study results demonstrated the efficiency of the PCM to control and to stabilize the indoor temperature with a high energy savings. Those results are very important for hot climate, because the PCM reduces the input heat flux when the temperature is high and it returns heat to the environment when the temperature decreases. For these reasons the good function of a PCM is related to the variable outdoor temperature. The choice of the best melting temperature value of the PCM is an important phase of a correct design, because the melting phase determines the start of the functioning of the PCM.

The design method in general is not very accurate because it is influenced by different causes: enthalpy temperature curve of the PCM (the factory does not always release an accurate curve), the WMO weather stations are not always nearby; the mathematical model is very complexed and the algorithm resolution gives approximate values. The PCM application (Caprara and Stoppiello, 2012) are not widespread in agrifood buildings for these reasons but the PCM in food storage buildings will be very important in the future because the control of temperature in storage stage is fundamental to obtain a high sustainable quality of the production. In fact the quality and the sustainability of food process depend on the building where the process is conducted (Barreca et al., 2014) (Barreca and Praticò, 2018). EVOO is appreciated by consumers for its unique sensory characteristics and high nutritional values, for these reasons, the olive oil industry has to monitor oil quality throughout the production line and has to be able to provide realistic information on quality considering the temperature changes during storage and distribution. In fact a correct storage system should forecast not only a temperature control but also a continuous monitoring of the quality of EVOO. This study has not reported the quality parameters of EVOO during the storage stage because the observation time was only for a few months. A future study will be carried out to evaluate the quality parameters of EVOO in a storage room with multilayer walls in PCM.

Allegato A — pagina 31 del documento originale

ALLEGATO B

Progetto di ricerca — Tetti ventilati in laterizio

Abstract

Several passive cooling design techniques are known for reducing solar heat gain through building envelope in summer season. These include the use of phase change materials (PCM), which has received an increased attention over the last years, and the strategy of increasing the above-sheathing ventilation (ASV) in ventilated roofs. However, few studies combine both technologies to maximise the building resilience in hot season. The effect of including a PCM layer into a ventilated roof is numerically analysed here in two different configurations: firstly, laid on the roof deck (PCM1 case) and, secondly, suspended in the middle of the ASV channel (PCM2 case). A computational fluid dynamics model was implemented to simulate airflow and heat transfer around and through the building envelope, under 3 days of extreme hot conditions in summer with high temperatures and low wind speed. Results showed slight differences in terms of mean temperatures at the different roof layers, although temperature fluctuations at deck in the PCM1 case were smaller than half of those estimated for the benchmark case. However, PCM2 configuration achieved a daily reduction of about 10 Wh/m^2 (18%) in building energy load with respect to the benchmark case, whilst PCM1 got only 4% due to the lower ventilation at night time. Therefore, a suspended PCM layer in the ASV channel would be a better measure in terms of energy performance than laid on the deck surface, although this last option significantly decreases thermal stress of the insulation layer.

Keywords: passive cooling technique; ventilated pitched roof; phase change material; computational fluid dynamics

*Corresponding author: michele.bottarelli@unife.it

Received 14 October 2019; revised 21 December 2019; editorial decision 14 January 2020; accepted 14 January 2020

Allegato B — pagina 33 del documento originale

1. INTRODUCTION

According to the International Energy Agency (IEA), the building sector is responsible for nearly 40% of final global energy consumption worldwide, with major components in heating, cooling, ventilation, etc. [1]. Although IEA has identified some opportunities for global building energy demand to decline from now to 2040, due to a more efficient scenario, it has also warned about the fast growing of cooling in buildings. In fact, it has predicted that energy demand for space cooling will more than triple by 2050, an increase especially concentrated in the hottest parts of the world [2].

In this context, different passive cooling techniques have received an increased attention over the last decades. A suitable selection of these techniques, which can be classified into heat protection, heat modulation and heat dissipation techniques [3], depends on many factors, such as climatic conditions, building space constraints and performance of the passive technique [4]. In heat protection techniques, the building is protected from direct solar gains by using shading devices, active vegetation,

International Journal of Low-Carbon Technologies 2020, 00, 1–9

doi:10.1093/ijlct/ctaa001 Advance Access publication

Allegato B — pagina 34 del documento originale

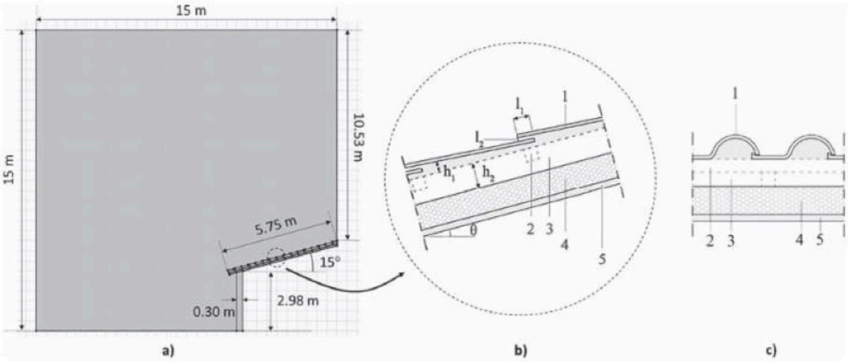

Figure 1. *(**a**) Sketch of the 2D model domain. (**b**) Simplified 2D model of the tile and ASV channel (benchmark case).* l_1*, length of tile overlap;* l_2*, thickness of gap between overlapping tiles;* h_1*, thickness of the air layer under the tile;* h_2 *thickness of the ventilation layer;* θ*, tilt angle. (**c**) Cross section of the Portuguese tile shape. 1, tiles; 2, battens and resulting air layer; 3, counter-battens and resulting air layer; 4, insulation layer; 5, wooden board.*

Table 1. *Geometric characteristics of the ventilated roof.*

Name	*Description*	*Value (unit)*
l	Tile thickness	0.01 (m)
l_1	Length of tile overlap	0.05 (m)
l_2	Distance between overlapping tiles	0.006 (m)
h_1	Thickness of air layer	0.015–0.03 (m)
h_2	Thickness of ventilation layer	0.08 (m)
θ	Tilt angle	15 (°)

etc. Regarding modulation techniques, the heat gain is modulated by the thermal inertia of the building structure. The integration of phase change materials (PCMs) in building envelope falls into this category. PCMs have high latent heat capacity and are able to absorb and release solar and infrared radiation through convection and radiation. They allow decreasing internal air temperature fluctuations [5] and reducing total discomfort hours and cooling energy loads [6]. It must be highlighted that that PCMs' performance depends on the quantity of the material and the temperatures during the day and night [7]. In heat dissipation techniques, excess heat of the building is released to a suitable environmental heat sink at a lower temperature. Within this group, roof ventilation, which uses environmental air as a heat sink, can also play an important role in lowering energy requirement for space cooling by increasing natural and forced air convection and reducing the heat transfer due to solar radiation.

Especially in hot climates, the roof plays an important role in comparison with other building elements due to its extension and exposure to the sun [8]. PCMs have been integrated in roofs in a variety of options with the aim of increasing thermal energy storage capacity of the building. In [9], a 3D heat transfer parametric study of a full-scale PCM roof is developed, in which different influencing factors on thermal performance (solar radiation, transition temperature, roof slope, etc.) were investigated. They observed a strong temperature delay in the room with respect to the common case and that roof slope, PCM layer thickness and absorption coefficient of external surfaces were the most relevant factors. In [10], a mathematical model is presented which was experimentally validated in order to predict the thermal behaviour of a roof made of brick and concrete with a middle PCM layer. Authors concluded that a double PCM layer could limit temperature swings and be suitable for all seasons. An experimental study is presented in [11] about a complex roof with PCM inserted into an enclosed air space between the corrugated iron roof and plasterboard. The air layer between the iron roof and the PCM was not ventilated. Authors proved that the PCM was able to store thermal energy in the daytime and released it at night. An experimental roof configuration that consisted of a combination of photovoltaic (PV) laminates, air cavities, fibreglass insulation with reflected foil facing and PCM heat sink is shown in [12]. Air cavities and air gap above the insulation layer provided above-sheathing ventilation (ASV), which helped to reduce cooling loads during summer. Over 50% of saving in cooling energy demand was achieved.

Different studies based on experimental and numerical approaches have also investigated the performance of ASV systems. Thus, laboratory tests were carried out to assess airflow and temperature distribution in ASV as functions of solar radiation and size and shape of the air channel [13]. A significant performance improvement over a standard ventilated roof was measured in full-scale models [14]. Numerical tools were used by other authors in order to estimate air distribution and heat transfer in ventilated roofs [8]. A numerical algorithm to predict heat, air and moisture transport in the building envelope and quantify the thermal benefits is developed in [15], around 14%, of using a tiled roof over a traditional shingle roof. A reduction between 30 and 50% of heat flux into the attic was reported by

Table 2. *Properties of building materials.*

Material	*Thickness (m)*	*Density (kg/m³)*	*Thermal conductivity (W/m·K)*	*Specific heat (J/kg·K)*	*Latent heat (J/kg)*	*Melting temperature (°C)*
Wall	0.30	850	0.20	840	—	—
Rockwool insulation layer	0.08	130	0.037	1030	—	—
Wooden board	0.02	450	0.15	2100	—	—
Tiles	0.01	2000	1.00	800	—	—
PCM ($Na_2CO_3 \cdot 10H_2O$)	0.02	1485 (solid) 1442 (liquid)	0.554 (solid)	1783	246.5	32 (span 2°C)
Backfill material	—	1200	0.8	1000	—	—

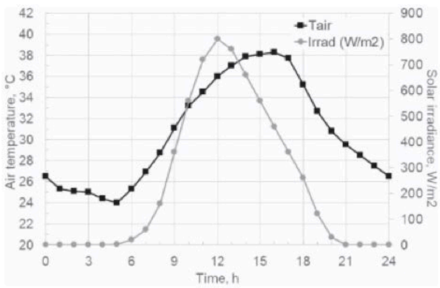

very few studies can be found in scientific literature on the combination of ASV and PCMs. Furthermore, to the best of the authors' knowledge, there are no studies on the use of ASV systems with increased air permeability together with PCM layers over the roof deck. Thus, the aim of the present work is to analyse the performance of this combination of passive techniques during hot periods in a Mediterranean site (Ferrara, Italy). Different configurations of ventilated roofs were simulated numerically by using CFD. First, a description of the methodology and case studies is given. Secondly, the numerical model is presented. Finally, the results obtained are analysed and discussed and conclusions drawn.

Figure 2. *Air temperature and solar irradiance for 1 day of the simulation period.*

other numerical studies when roof ventilation was considered in [16–18]. In [16], a new algorithm to predict free laminar convection heat transfer in ventilated roofs and also apply a 2D steady state computational fluid dynamics (CFD) modelling is created, from which they made a correlation to estimate naturally induced airflow within the ventilated space. In [17], a 1D heat transfer steady-state mathematical model is developed as based on thermal resistance circuits. In [18], a 2D steady-state CFD model is used to study the performance of the ventilated roof for different configurations, and it was concluded that the best results were obtained when placing the insulation layer under the air layer. These numerical studies neglected the tile air permeability between the overlapping tiles and modelled ASV as an air duct. Air permeability was experimentally analysed in [19], where it is concluded that, in the roofs studied, air permeability and the introduction of building elements which obstruct the flow could counter any differences in performance correlated with the cross section of the ventilation duct. The enhancement of ASV by tile air permeability was experimentally and numerically studied in the European project LIFE HEROTILE (LIFE14CCA/IT/000939), in which a significant increase in ASV using new tile designs was achieved [20–22].

Recent studies generally focus on the combination of different passive cooling technologies in order to maximise the building cooling potential and energy-saving capabilities [23]. However,

2. METHODOLOGY

The simulation of airflow and heat transfer in ventilated roofs is a complex problem that involves turbulence with a variety of length scales. Larger scales, which are related to wind and wind–building interaction, are connected to the small scales of the flow within the ASV and the tiny interstices among the overlapping tiles [8]. In order to solve this problem, CFD numerical simulations of the heat transfer mechanisms and airflow over a real building and through its ventilated pitched tiled roof has been considered here. The commercial finite-element code COMSOL Multiphysics V5.3 was used. A reference or benchmark case study in which only the ASV was taken into account was used for comparison with other configurations that also included a PCM layer over the roof deck. The descriptions of the CFD model and study cases are given next.

2.1. CFD model

2.1.1. *Domain*

As the main interest is focussed on the natural ventilation channel and heat transfer exchange in the roof of the building, a 2D domain was considered as a section of a one-floor building of infinite width, neglecting 3D effects of wind–building interaction. A sketch of the domain is shown in Figure 1a). The building, for which only one half has been considered, is covered by a pitched roof with a slope of 15° and is included in a 15 m × 15 m external air environment. Details of the roof are given in Figure 1b and c (benchmark case). The roof covering is made of Portuguese roof

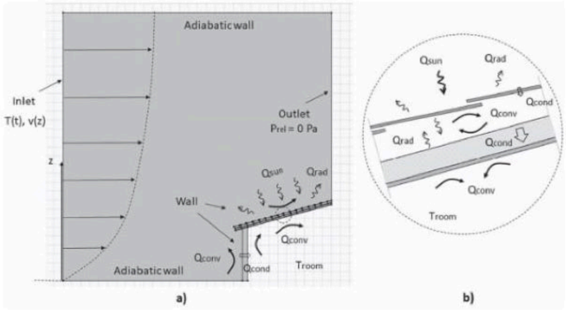

Figure 3. *(**a**) Description of boundary conditions in the whole domain. (**b**) Details of boundary conditions on the roof. t, time; T, temperature; z, height; v, wind speed; P_{rel}, relative pressure; Q_{sun}, solar irradiance; Q_{rad}, radiation heat flux; Q_{conv}, convective heat flux; Q_{cond}, conductive heat flux; T_{room}, fixed room air temperature.*

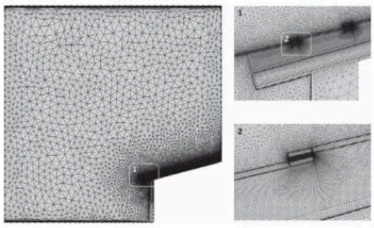

Figure 4. *Details of the mesh used to represent the whole domain and ASV channel (benchmark case).*

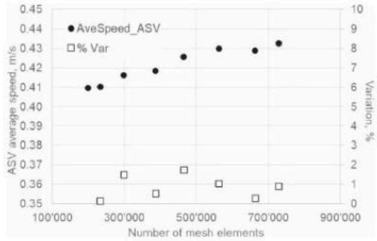

Figure 5. *Mesh independence study. Average air speed at the cross section in the middle of the ASV channel was used for comparison (benchmark case).*

39

Allegato B — pagina 39 del documento originale

tiles laid on a batten and counter-batten system. In the present study, the batten and counter-batten system is not included in the model and tile shape is simplified such that the resulting ASV and tile models are as shown in Figure 1b [8]. Air will flow into the ventilation channel at the eaves and through the gaps among the tiles, and mainly leaving out at the ridge.

Geometric values of the roof elements and properties of the building materials are described in Tables 1 and 2, respectively.

In Table 2, properties of the PCM ($Na_2CO_3{\cdot}10H_2O$, an hydrated salt) used in the present study are reported, as given in [24]. Hydrated salts are often preferred in building applications due to their high latent heat combined to a low price. A mixture of a backfill material (20% of total volume) and the PCM is considered in the PCM layer that will be integrated in other ASV configurations. To represent time dependence of mixture density, conductivity and specific heat during the phase change, some specific relationships expressed in terms of normalised Dirac's pulse and different step functions were implemented, as reported in [25].

2.1.2. *Boundary conditions*

The numerical study of the energy performance of the ASV system was developed for a period of three summer days with extreme hot conditions, that is, high air temperatures and high solar irradiance (W/m^2) (Figure 2). Minimum and maximum daily air temperatures were 24.0 and 38.3°C, respectively. A time-dependent air temperature ($T(t)$) was set as a boundary condition at the inlet of the fluid domain. Furthermore, solar irradiance, which reached a maximum value of 800 W/m^2, was set as an input time-dependent heat flux over the roof of the building. Roof surface had a hemispherical reflectance of 0.3.

40

Allegato B — pagina 40 del documento originale

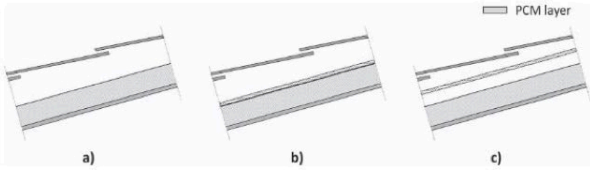

Figure 6. *Cross sections of the ventilated roofs for the three case studies: (**a**) benchmark case (BM); (**b**) PCM layer laid on the roof deck (PCM1); (**c**) PCM layer hanging in the middle of the ASV channel (PCM2).*

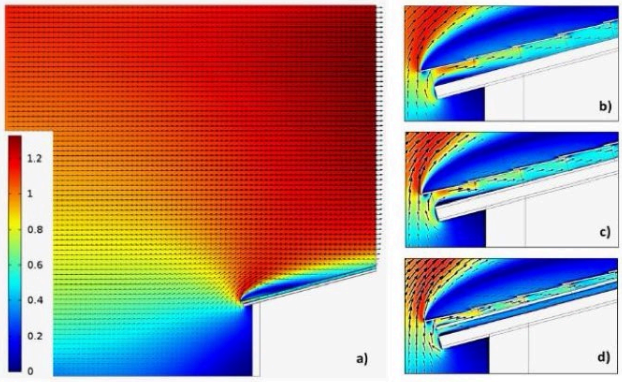

Figure 7. *Surface and vector velocity plots. (**a**) Full domain (BM). Details of the same plot for the different case studies: (**b**) BM, (**c**) PCM1 and (**d**) PCM2.*

Allegato B — pagina 41 del documento originale

A potential wind velocity profile was also set at the inlet, with a speed of 1 m/s (v_0) at a reference level of 10 m (z_0). This profile followed the following power law:

$$v(z) = v_0\left(\frac{z}{z_0}\right)^{\alpha}$$ Equation 1: Wind speed profile

where:

- $v(z)$ = wind speed at height z (m/s)
- z = height (m)
- v_0 = wind speed at a reference height (z_0) (m/s)
- z_0 = reference height (z_0) (m)
- α = empirical non-dimensional exponent

The exponent α, which depends on the surface roughness, was set to 0.3, a typical value for urban areas [26]. Thus, low wind speed conditions, for which the efficiency of the ASV systems is smaller, will be analysed. Also, these conditions would be more similar to the real ones in which the air in the streets does not flow in a direction perpendicular to the building façade.

Constraints at other boundaries of the domain are described in Figure 3. Details of the different heat transfer mechanisms and conditions considered in the ventilated roof are shown in Figure 3b. A constant room air temperature of 26°C and a heat transfer coefficient of 8 W/(m^{2}K) were set on the ceiling and inside surface of the building wall. Grey body and surface-to-surface radiation models were used to calculate radiation heat transfer between surfaces in the ASV channel.

2.1.3. *Mesh independence*

An unstructured triangular mesh has been used with inflation layers (prismatic layers of increasing thickness) in the proximity

Allegato B — pagina 42 del documento originale

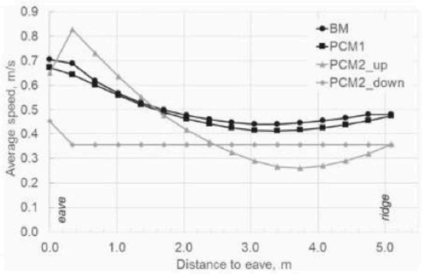

Figure 8. *Average speed at different cross sections along the ASV channel.*

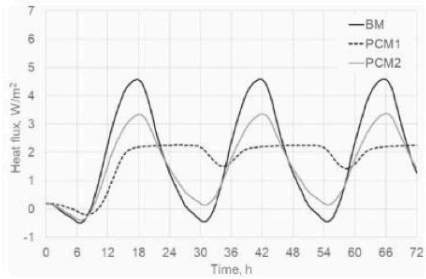

Figure 10. *Time dependence of heat flux (W/m²) through the ceiling.*

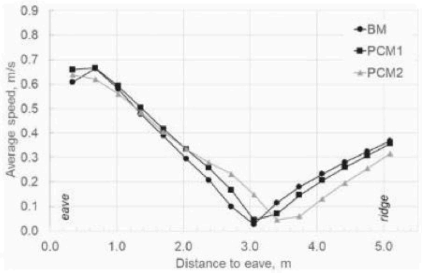

Figure 9. *Average speed at the outlet cross sections of the inter-tile gaps.*

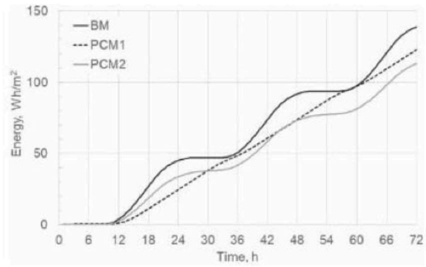

Figure 11. *Time dependence of energy (Wh/m²) entering the room through the ceiling. Numerical integration of curves in Figure 10 for positive values of heat flux.*

to the wall–air interfaces in order to capture gradients within the mechanical and thermal boundary layers (Figure 4). Several runs of the initial CFD model were performed on different size meshes, and their results were compared to analyse the grid independence of the solution. The average air speed at the cross section in the middle of the ASV channel was used for comparison. Although there were no great differences (around 1.5% of relative variation) (Figure 5), meshes of near half a million elements were built for all the case studies developed.

2.1.4. *Turbulence model and solving strategy*

The k–ε model with standard wall functions was used to simulate turbulence within the fluid domain. The problem was solved in two stages. First, a steady-state solution of the airflow was sought in the thermal conditions formerly described. Then, from the steady-state airflow solution, the heat transfer transient problem was solved. This strategy can be justified considering that temperature differences along the roof are not very high and, consequently, airflow through the ASV channel is mainly dependent on external wind conditions. A relative tolerance of 10^{-3} was set for residuals.

2.2. Case studies

Three case studies were considered: a benchmark case (from now on 'BM') described in Section 2.1 and two configurations (PCM1 and PCM2) in which the ASV system was coupled with a PCM layer over the roof deck. In the last two cases, a 2-cm-thick PCM layer was considered. In PCM1 configuration, the layer was laid on the roof deck whilst in PCM2 the layer was suspended in the middle of the ASV channel (Figure 6).

Meshes with 497249, 487982 and 358988 elements were built for the BM, PCM1 and PCM2 case studies, respectively.

3. RESULTS AND DISCUSSION

Although authors have mainly focussed their attention on heat transfer through the different roof configurations, a study on velocity field has also been carried out in order to check the right performance of the numerical simulations. Thus, Figure 7 shows the airflow in the whole domain and through the ASV channel for the three case studies. In terms of velocity field, BM and PCM1

Table 3. *Temperature at different sections (1, 8 and 16) of the outer surface of the insulation layer.*

(°C)	S1 BM	S1 PCM1	S1 PCM2	S8 BM	S8 PCM1	S8 PCM2	S16 BM	S16 PCM1	S16 PCM2
T_{MEAN}	30.5	30.2	30.4	30.6	30.1	30.0	31.2	30.6	29.9
T_{MIN}	24.3	25.0	24.4	24.3	25.4	24.6	24.4	25.5	24.9
T_{MAX}	37.1	31.6	36.9	37.5	31.4	35.0	39.1	31.5	33.5
$T_{MAX} - T_{MIN}$	12.8	6.6	12.6	13.2	6.0	10.4	14.7	6.0	8.6

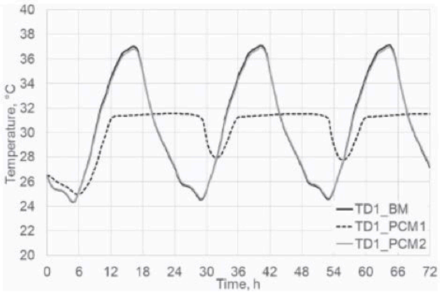

Figure 12. *Temperatures at the first part (D1, close to the eave) on the deck (insulation layer) surface.*

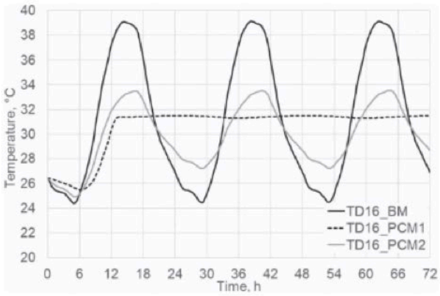

Figure 14. *Temperatures at the last part (D16, close to the ridge) on the deck surface.*

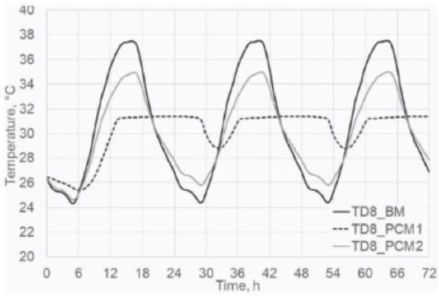

Figure 13. *Temperatures at the middle part (D18) on the deck surface.*

show a very similar behaviour, with a decay of air speed in the middle part of the channel and a slight increase towards the ridge. This dependence has been experimentally observed in [8]. The highest values of air speed at the beginning can be explained by the action of the eave edge that channels air coming from below.

Regarding PCM2, airflow is split into two streams by the suspended PCM layer. It is interesting to note that, whilst the upper flow behaves similarly to the former two cases, the flow below the PCM layer shows an almost uniform velocity distribution. This is also shown in Figure 8 and can be explained again by the action of the eave edge and the irregularities caused by inter-tile gaps. The uniformity of velocity under the PCM layer is caused by the even distribution of surfaces. Figure 9 provides the values of the average velocity at the different outlet cross sections of the inter-tile gaps. A very similar trend is seen for the three cases with a steep decrease to nearly null velocity near the middle of the roof, which is related to the stagnation area in the wake of the outer flow and to an indoor–outdoor pressure balance.

Temperature has been estimated in many different locations of the building roof: on the ceiling (inner surface of the wooden board), at the interface between the wooden board and the insulation layer, over the insulation layer, on the PCM surfaces, etc. Thus, the average temperature of the ceiling and at the interface between the wooden board and the insulation layer are almost identical for the three cases, around 26.2 and 26.7°C, respectively. Also, the average temperature at the outer surface of the insulation layer is very similar, with a value that ranges from 30.0°C (PCM2) to 30.6°C (BM). At this interface, temperature variations seem to be smaller for the PCM1 configuration.

Regarding the heat transfer through the roof, mean values of heat flux for BM, PCM1 and PCM2 cases are 1.9, 1.7 and 1.5 W/m², respectively. Thus, a 20% reduction is achieved with PCM2 configuration. Although a clear dampening is observed in the time dependence of heat flux, it seems that PCM1 performance is not very good, probably because PCM is not able to release upwards the required amount of heat at night (Figure 10). In fact, the energy transferred to the room after a period of 24 h is almost the same (a difference of around 4%) for BM and PCM1 configurations (Figure 11). In the same period, a reduction in building energy load of about 10 Wh/m^2 (18%) is achieved by PMC2 configuration with respect to the benchmark case. This better performance of the PCM2 configuration may be explained by the ventilation of the two surfaces of the PCM layer, which enhances heat release.

An interesting location, from the construction and refurbishment perspective, is the outer surface of the insulation layer because it degrades under extreme temperature conditions. Thus, surface temperature at different sections of the deck has been compared among the three case studies. The ASV channel was divided into 16 sections (related to the 16 tiles of the half of the roof). Thus, temperatures at Sections 1 (at the eave), 8 and 16 (at the ridge) on the deck surface have been analysed (Table 3). The smallest temperature fluctuations (half of those estimated for the BM case) and the lowest maximum temperature values were obtained with PCM1 configuration, that is, with the PCM layer right over the insulation layer.

As it can be seen from Figures 12–14, temperature on the whole deck surface is almost constant for PCM1 configuration (32°C, the melting point of the PCM). Furthermore, the dampening effect of the PCM layer in PCM2 configuration increases far from the eaves.

Although some of the results presented here have been observed experimentally, e.g. the velocity distribution within the ASV channel, future developments will involve the experimental confirmation of the issues and conclusions drawn by the energy performance numerical simulations.

REFERENCES

[1] IEA, 2019. IEA website: https://www.iea.org/topics/energyefficiency/buildings/

[2] IEA. 2018. The future of cooling. In *Opportunities for Energy-Efficient Air Conditioning*. OECD/IEA.

[3] Santamouris M, Kolokotsa D. Passive cooling dissipation techniques for buildings and other structures: The state of the art. *Energ Buildings* 2013;**57**:74–94.

[4] Bhamare DK, Rathod MK, Banerjee J. Passive cooling techniques for building and their applicability in different climatic zones—The state of art. *Energ Buildings* 2019;**198**:467–90.

[5] Sari A, Alkan C, Özcan AN. Synthesis and characterization of micro/nano capsules of PMMA/capric-stearic acid eutectic mixture for low temperature-thermal energy storage in buildings. *Energ Buildings* 2015;**90**:106–13.

[6] Sajjadian SM, Lewis J, Sharples S. The potential of phase change materials to reduce domestic cooling energy loads for current and future UK climates. *Energ Buildings* 2015;**93**:83–9.

4. CONCLUSIONS

In this work, the authors have studied the performance of a combination of two passive cooling techniques: ASV systems and the use of PCM on a pitched tiled roof of a building. They used CFD with finite elements (COMSOL, v5.3) to develop numerical simulations under extreme hot conditions in a Mediterranean site (Ferrara, Italy). Three case studies were considered: a benchmark case (BM) with only the natural ventilation system on the building roof; a second study (PCM1) in which a PCM layer was laid over the roof deck; and a third one (PCM2) with the same PCM layer suspended in the middle of the ASV channel. Weather conditions were characterised by high temperatures and solar irradiance, with peak values of 38°C and 800 W/m^2, respectively. A typical urban potential wind profile with a reference value of 1 m/s (at 10 m) at the inlet of the domain was taken into account. These low values of air speed would also resemble real urban situations in which street wind is not usually perpendicular to the building façade. k–ε with wall functions was used to model turbulence. A mesh independence study, in which the average air speed at the cross section in the middle of the ASV channel was used for comparison, was also developed.

It can be concluded that the PCM1 case slightly reduces building energy load (about 4%) with respect to the BM case in a 24-h period of time. In contrast, PCM2 configuration gets a reduction of about 18% (10 Wh/m^2) in the same period. A study on surface temperature on the insulation layer (deck) revealed that the PCM1 case got an almost constant value, thus avoiding high fluctuations and delaying material degradation.

[7] Zalba B, Marín JM, Cabeza LF, Mehling H. Review on thermal energy storage with phase change: Materials, heat transfer analysis and applications. *Appl Therm Eng* 2003;**23**:251–83.

[8] Bortoloni M, Bottarelli M, Piva S. Summer thermal performance of ventilated roofs with tiled coverings. *J Phys Conf* 2017;**796**:1–10.

[9] Dong L, Yumeng Z, Changyu L, Guozhong W. Numerical analysis on thermal performance of roof contained PCM of a single residential building. *Energ Convers Manage* 2015;**100**:147–56.

[10] Pasupathy A, Velraj R. Effect of double layer phase change material in building roof for year round thermal management. *Energ Buildings* 2008;**40**:193–203.

[11] Guichard S, Miranville F, Bigot D *et al.* Experimental investigation on a complex roof incorporating phase-change material. *Energ Buildings* 2015;**108**:36–43.

[12] Kosny J, Biswas K, Miller W, Kriner S. Field thermal performance of naturally ventilated solar roof with PCM heat sink. *Sol Energy* 2012;**86**: 2504–14.

[13] Lee S, Park SH, Yeo MS, Kim KW. An experimental study on airflow in the cavity of a ventilated roof. *Build Environ* 2009;**44**:1431–9.

[14] Dimoudi A, Androutsopoulos A, Lykoudis S. Summer performance of a ventilated roof component. *Energ Buildings* 2006;**38**:610–7.

[15] De With G, Cherry N, Haig J. Thermal benefits of tiled roofs with above-sheathing ventilation. *Int J Building Phys* 2009;**33**:171–94.

[16] Miller, W.A., Keyhani, M., Stovall, T., 2007. Natural convection heat transfer in roofs with above-sheathing ventilation. Thermal performance of the exterior envelopes of buildings, X, proceedings of ASHRAE THERM X, Clearwater, FL

[17] Ciampi M, Leccese F, Tuoni G. Energy analysis of ventilated and microventilated roofs. *Sol Energy* 2005;**79**:183–92.

[18] Gagliano A, Patania F, Nocera F *et al.* Thermal performance of ventilated roofs during summer period. *Energ Buildings* 2012;**49**:611–8.

[19] D'Orazio M, Di Perna C, Principi P, Stazi A. Effects of roof tile permeability on the thermal performance of ventilated roofs: Analysis of annual performance. *Energ Buildings* 2008;**40**:911–6.

[20] High Energy savings in building cooling by ROof TILEs shape optimization toward a better above sheathing ventilation (Life Herotile project). http://www.lifeherotile.eu/it/

[21] Bottarelli M, Bortoloni M, Dino G. Experimental analysis of an innovative tile covering for ventilated pitched roofs. *Int J Low Carbon Tec* 2017;**13**:6–14.
[22] Bottarelli M, Bortoloni M, Zannoni G *et al.* CFD analysis of roof tile coverings. *Energy* 2017;**137**:391–8.
[23] Roman KK, O'Brien T, Alvey JB, Woo OJ. Simulating the effects of cool roof and PCM (phase change materials) based roof to mitigate UHI (urban heat island) in prominent US cities. *Energy* 2016;**96**:103–17.
[24] Cabeza LF, Castell A, Barrenechea C *et al.* Materials used as PCM in thermal energy storage in buildings: A review. *Renew Sust Energ Rev* 2011;**15**:1675–95.
[25] Bottarelli M, Bortoloni M, Su Y *et al.* Numerical analysis of a novel ground heat exchanger coupled with phase change materials. *Appl Therm Eng* 2015;**88**:369–75.
[26] Masters GM. 2004. *Renewable and Efficient Electric Power Systems*. New York: John Wiley and Sons.

Allegato B — pagina 49 del documento originale

ALLEGATO C

Simulazione termica dinamica IDA ICE — edificio DEMO CNR di Pisa

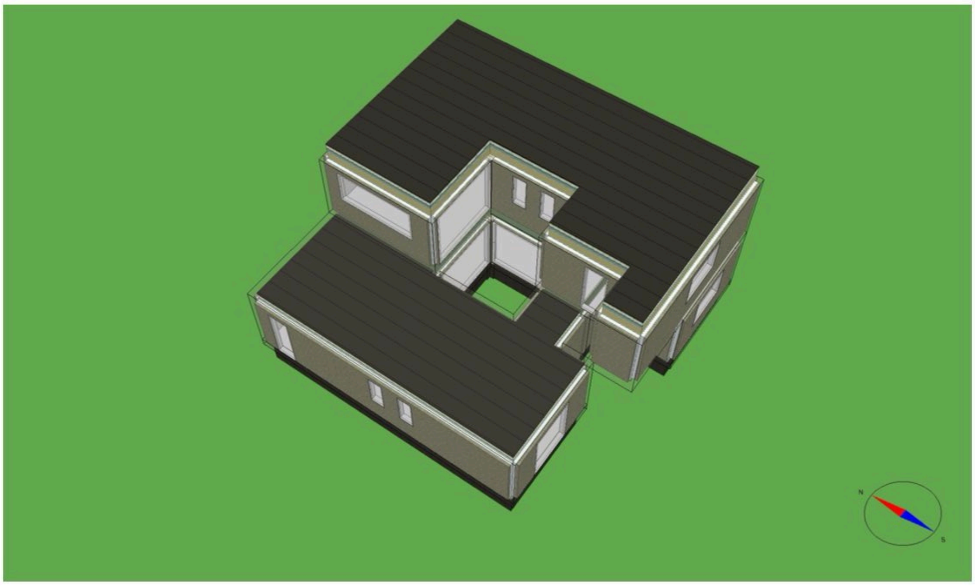

71

Allegato C — pagina 71 del documento originale

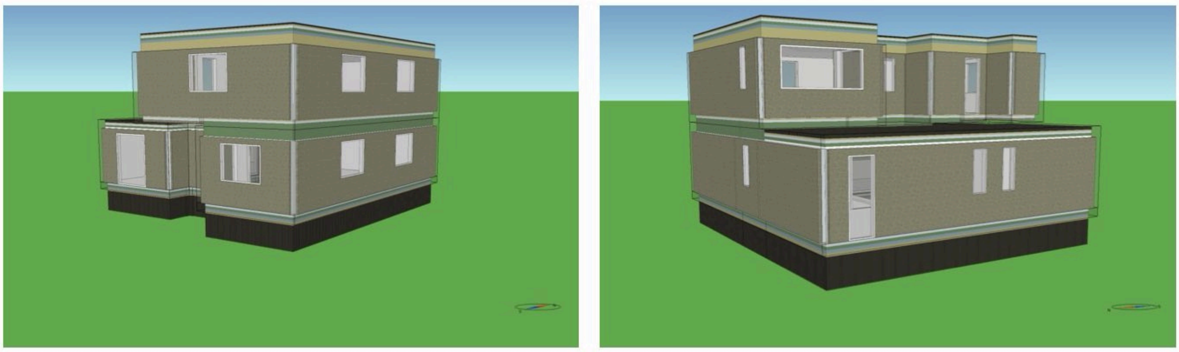

72

Allegato C — pagina 72 del documento originale

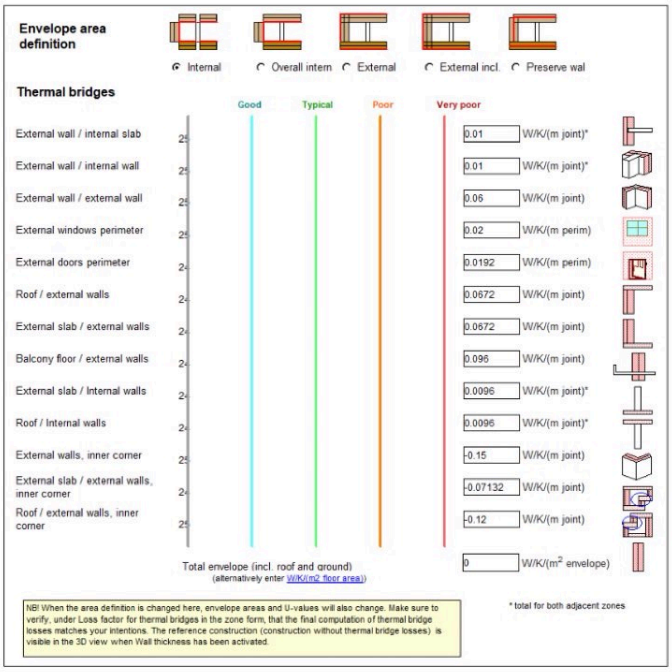

73

Allegato C — pagina 73 del documento originale

EQUA SIMULATION TECHNOLOGY GROUP

Input data Report

Project		Building	
		Model floor area	213.3 m²
Customer		Model volume	575.8 m³
Created by	Massimo Salerno	Model ground area	130.1 m²
Location	Pisa/S. Giusto_161580 (ASHRAE 2013)	Model envelope area	579.8 m²
Climate file	[Default]	Window/Envelope	13.4 %
Case	MODELLO ESTATE FUNZIONANTE	Average U-value	0.2998 W/(m² K)
Simulated	04/05/2022 12:50:04	Envelope area per Volume	1.007 m²/m³

Wind driven infiltration airflow rate 79.959 l/s at 50.000 Pa

Building envelope	Area [m²]	U [W/(m² K)]	U*A [W/K]	% of total
Walls above ground	**227.79**	**0.17**	**38.57**	**22.19**
EXT WALL CNR PISA MAGGIO PCM 23	227.79	0.17	38.57	22.19
Walls below ground	**0.00**	**0.00**	**0.00**	**0.00**
Roof	**137.48**	**0.15**	**20.78**	**11.95**
COPERTURA PISA CNR pcm25	84.43	0.14	12.14	6.98
TETTO VERDE PISA CNR	53.04	0.16	8.64	4.97
Floor towards ground	**130.15**	**0.09**	**12.00**	**6.90**
SOLAIO TERRENO CRN PISA	130.15	0.09	12.00	6.90
Floor towards amb. air	**6.97**	**0.20**	**1.38**	**0.79**
SOLAIO LOGGIA CNR PISA	6.97	0.20	1.38	0.79
Windows	**77.42**	**1.16**	**90.04**	**51.79**
PATIO CNR PISA	77.42	1.16	90.04	51.79
Doors	**0.00**	**0.00**	**0.00**	**0.00**
Thermal bridges			**11.09**	**6.38**
Total	**579.80**	**0.30**	**173.85**	**100.00**

74

Allegato C — pagina 74 del documento originale

Thermal bridges	Area or Length	Avg. Heat conductivity	Total [W/K]
External wall / internal slab	78.14 m	0.005 W/(m K)	0.391
External wall / internal wall	24.30 m	0.005 W/(m K)	0.122
External wall / external wall	35.10 m	0.060 W/(m K)	2.106
External windows perimeter	160.90 m	0.020 W/(m K)	3.218
External doors perimeter	0.00 m	0.000 W/(K m)	0.000
Roof / external walls	75.25 m	0.067 W/(m K)	5.057
External slab / external walls	72.77 m	0.067 W/(m K)	4.890
Balcony floor / external walls	0.00 m	0.000 W/(K m)	0.000
External slab / Internal walls	0.48 m	0.005 W/(m K)	0.002
Roof / Internal walls	9.01 m	0.005 W/(m K)	0.043
External walls, inner corner	24.30 m	-0.150 W/(m K)	-3.645
Roof / external walls, inner corner	6.48 m	-0.120 W/(m K)	-0.778
External slab / external walls, inner corner	4.41 m	-0.071 W/(m K)	-0.315
Total envelope (incl. roof and ground)	577.63 m^2	0.000 W/(m^2 K)	0.000
Extra losses	-	-	0.000
Sum	-	-	11.091

Windows	Area [m^2]	U Glass [W/(m^2 K)]	U Frame [W/(m^2 K)]	U Total [W/(m^2 K)]	U*A [W/K]	Shading factor g
N	5.25	1.07	2.00	1.16	6.10	0.35
E	20.22	1.07	2.00	1.16	23.51	0.35
S	27.70	1.07	2.00	1.16	32.21	0.35
W	24.27	1.07	2.00	1.16	28.22	0.35
Total	77.42	1.07	2.00	1.16	90.04	0.35

Air handling unit	Pressure head supply/exhaust [Pa/Pa]	Fan efficiency supply/exhaust [-/-]	System SFP [kW/(m^3/s)]	Heat exchanger temp. ratio/min exhaust temp. [-/C]
Mixing box (recirculation)	160.00/40.00	0.80/0.50	0.20/0.08	0.00/0.00

DHW use	L/per occupant and day	No. of persons	Total, [l/s]
	0.000	21.000	0.000

75

Allegato C — pagina 75 del documento originale

EQUA SIMULATION TECHNOLOGY GROUP		**Delivered Energy Report**	
Project		**Building**	
		Model floor area	213.3 m^2
Customer		Model volume	575.8 m^3
Created by	Massimo Salerno	Model ground area	130.1 m^2
Location	Pisa/S. Giusto_161580 (ASHRAE 2013)	Model envelope area	579.8 m^2
Climate file	[Default]	Window/Envelope	13.4 %
Case	MODELLO INVERNO FUNZIONANTE	Average U-value	0.2998 W/(m^2 K)
Simulated	04/05/2022 12:25:47	Envelope area per Volume	1.007 m^2/m^3

Building Comfort Reference

Percentage of hours when operative temperature is above 27°C in worst zone	0 %
Percentage of hours when operative temperature is above 27°C in average zone	0 %
Percentage of total occupant hours with thermal dissatisfaction	92 %

Delivered Energy Overview

	Purchased energy		Peak demand
	kWh	kWh/m^2	kW
Lighting, facility	34	0.2	0.06
Electric cooling	0	0.0	0.0
HVAC aux	262	1.2	0.33
Electric heating	442	2.1	5.67
Total, Facility electric	738	3.5	
Domestic hot water	0	0.0	0.0
Total, Facility fuel*	0	0.0	
Total	738	3.5	
Equipment, tenant	347	1.6	0.32
Total, Tenant electric	347	1.6	
Grand total	1085	5.1	

*heating value

76

Allegato C — pagina 76 del documento originale

Monthly Purchased/Sold Energy

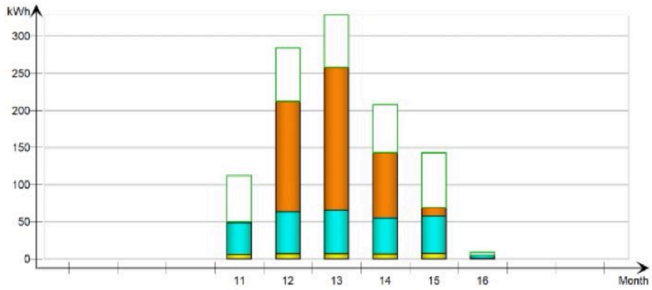

Month	Facility electric				Facility fuel (heating value)	Tenant electric
	Lighting, facility	Electric cooling	HVAC aux	Electric heating	Domestic hot water	Equipment, tenant
	(kWh)	(kWh)	(kWh)	(kWh)	(kWh)	(kWh)
11	6.0	0.0	43.0	1.6	0.0	61.8
12	6.9	0.0	56.6	148.6	0.0	72.0
13	6.9	0.0	58.6	192.2	0.0	70.7
14	6.3	0.0	48.9	88.2	0.0	64.8
15	7.2	0.0	50.3	11.4	0.0	73.8
16	0.4	0.0	4.7	0.0	0.0	4.2
Total	33.6	0.0	262.1	442.0	0.0	347.3

IDA Indoor Climate and Energy
Version: 4.802
License: IDA40:8888

Allegato C — pagina 77 del documento originale

Used energy

kWh (sensible and latent)

Month	Zone heating	Zone cooling	AHU heating	AHU cooling	Dom. hot water
11	2.3	0.0	0.0	0.0	0.0
12	215.9	0.0	0.0	0.0	0.0
13	279.1	0.0	0.0	0.0	0.0
14	128.0	0.0	0.0	0.0	0.0
15	16.6	0.0	0.0	0.0	0.0
16	0.0	0.0	0.0	0.0	0.0
Total	641.9	0.0	0.0	0.0	0.0

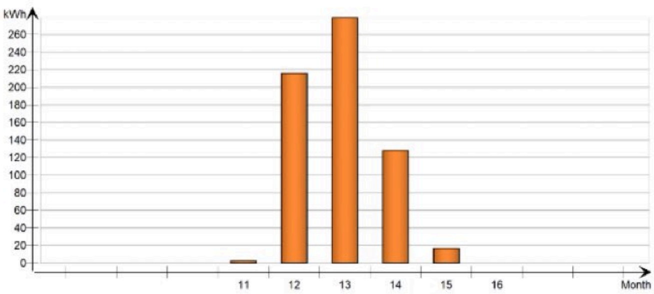

Allegato C — pagina 78 del documento originale

Utilized free energy

kWh (sensible and latent)

Month	AHU heat recovery	AHU cold recovery	Plant heat recovery	Plant cold recovery	Solar heat	Ground heat	Ground cold	Ambient heat	Ambient cold
11	9890.0	0.0							
12	10575.0	0.0							
13	10609.0	0.0							
14	9543.0	0.0							
15	11405.0	0.0							
16	972.9	0.0							
Total	52994.9	0.0							

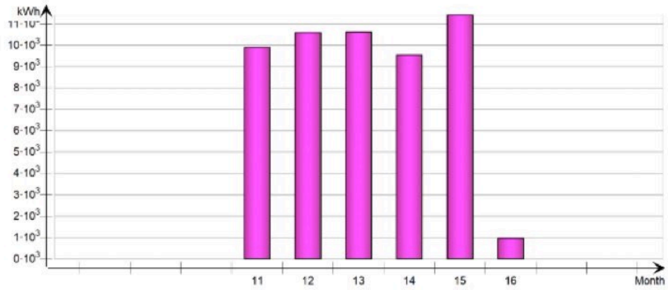

79

Allegato C — pagina 79 del documento originale

Auxiliary energy

kWh

Month	Humidification	Fans	Pumps
11		42.9	0.0
12		49.7	0.4
13		49.7	0.5
14		44.8	0.2
15		49.7	0.0
16		4.7	0.0
Total		241.7	1.2

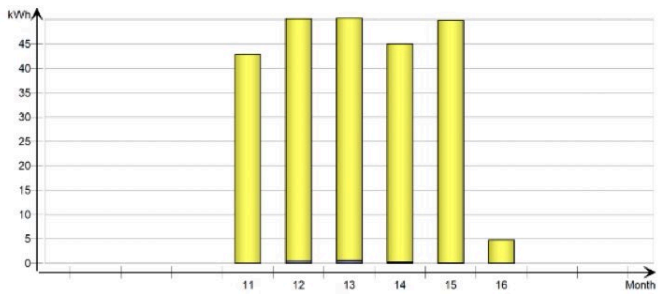

80

Allegato C — pagina 80 del documento originale

Building Comfort Reference

Percentage of hours when operative temperature is above 27°C in worst zone	34 %
Percentage of hours when operative temperature is above 27°C in average zone	21 %
Percentage of total occupant hours with thermal dissatisfaction	45 %

Delivered Energy Overview

	Purchased energy		Peak demand
	kWh	kWh/m²	kW
Lighting, facility	38	0.2	0.06
Electric cooling	1398	6.6	6.24
HVAC aux	167	0.8	0.49
Electric heating	0	0.0	0.0
Total, Facility electric	1603	7.5	
Domestic hot water	0	0.0	0.0
Total, Facility fuel*	0	0.0	
Total	1603	7.5	
Equipment, tenant	388	1.8	0.32
Total, Tenant electric	388	1.8	
Grand total	1991	9.3	

*heating value

Allegato C — pagina 81 del documento originale

Monthly Purchased/Sold Energy

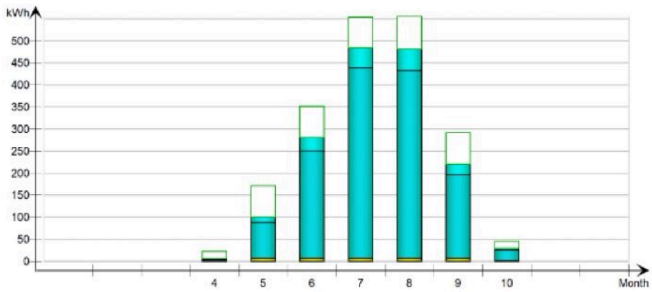

Month	Facility electric				Facility fuel (heating value)	Tenant electric
	Lighting, facility	Electric cooling	HVAC aux	Electric heating	Domestic hot water	Equipment, tenant
	(kWh)	(kWh)	(kWh)	(kWh)	(kWh)	(kWh)
4	1.6	3.4	1.4	0.0	0.0	16.2
5	6.9	81.1	12.3	0.0	0.0	70.8
6	6.9	243.9	30.2	0.0	0.0	70.8
7	6.6	431.9	45.7	0.0	0.0	69.1
8	7.2	425.9	48.4	0.0	0.0	73.8
9	6.9	188.6	24.6	0.0	0.0	70.8
10	1.6	23.7	4.2	0.0	0.0	16.2
Total	37.5	1398.5	166.8	0.0	0.0	387.9

Allegato C — pagina 82 del documento originale

Used energy

kWh (sensible and latent)

Month	Zone heating	Zone cooling	AHU heating	AHU cooling	Dom. hot water
4	0.0	0.0	0.0	8.6	0.0
5	0.0	0.0	0.0	202.6	0.0
6	0.0	17.9	0.0	591.8	0.0
7	0.0	49.9	0.0	1030.0	0.0
8	0.0	116.9	0.0	947.8	0.0
9	0.0	4.7	0.0	466.8	0.0
10	0.0	0.0	0.0	59.2	0.0
Total	0.0	189.5	0.0	3306.8	0.0

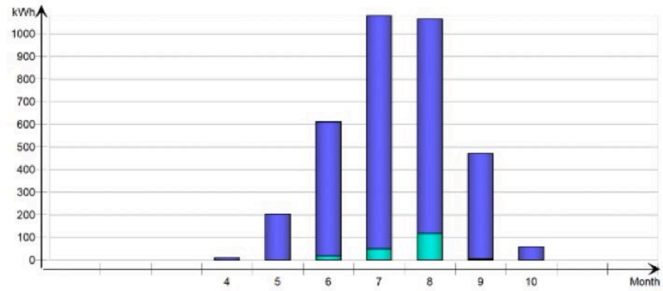

83

Allegato C — pagina 83 del documento originale

Utilized free energy

kWh (sensible and latent)

Month	AHU heat recovery	AHU cold recovery	Plant heat recovery	Plant cold recovery	Solar heat	Ground heat	Ground cold	Ambient heat	Ambient cold
4	120.4	0.0							
5	183.2	0.0							
6	632.2	0.0							
7	1429.0	0.0							
8	1754.0	0.0							
9	262.9	0.0							
10	43.8	0.0							
Total	4425.5	0.0							

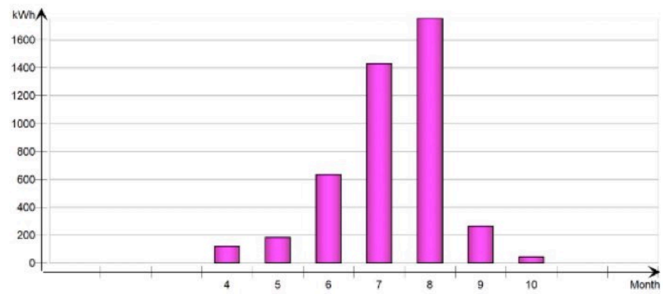

84

Allegato C — pagina 84 del documento originale

Auxiliary energy

kWh

Month	Humidification	Fans	Pumps
4		1.4	0.0
5		11.7	0.6
6		28.0	1.7
7		41.2	3.0
8		42.0	2.8
9		23.1	1.3
10		4.0	0.2
Total		151.4	9.7

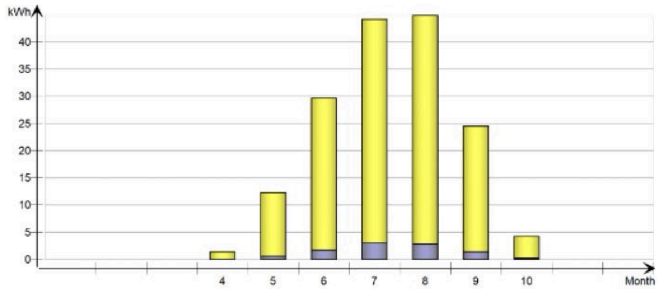

85

Allegato C — pagina 85 del documento originale

ALLEGATO D

Test di laboratorio e tavole tecniche

ALCUNI ESEMPI DI APPLICAZIONE IN PARETE (Protezione da sovratemperatura esterna)

1 intonaco interno - 2 isolante termico - 3 strato di PCM - 4 intonaco esterno

GIORNO lo strato di PCM assorbe il flusso termico dovuto all'assorbimento della radiazione solare e alla differenza di temperatura dell'aria

NOTTE la maggior parte dell'energia termica accumulata viene ceduta all'ambiente esterno

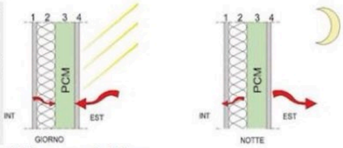

1° Modello funzionale di parete contenente materiali in passaggio di fase

1 intonaco interno - 2 isolante termico - 3 intercapedine ventilata - 4 strato diPCM - 5 intonaco esterno

GIORNO lo strato diPCM assorbe il flusso termico dovuto all'assorbimento della radiazione solare

NOTTE il calore va verso la parte esterna della parete e rimosso dall'aria all'interno dell'intercapedine

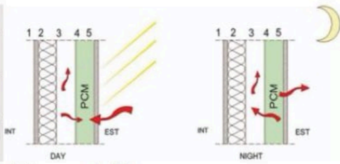

2° modello funzionale di parete contenente materiali in passaggio di fase

1 intonaco interno - 2 isolante termico - 3 strato di PCM - 4 intercapedine ventilata - 5 intonaco esterno

GIORNO lo strato diPCM assorbe il flusso termico dovuto all'assorbimento della radiazione solaree alla differenza di temperatura dell'aria

NOTTE la maggior parte del calore fluisce attraverso la parte esterna, rimosso per ventilazione naturale nella intercapedine

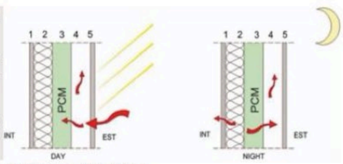

3° modello funzionale di parete contenente materiali in passaggio di fase

129

Allegato D — pagina 129 del documento originale

Test di laboratorio – Test di flusso termico - R3.3 (R = 3.3 m2.K/W) Verifica con e senza TI-SKIN

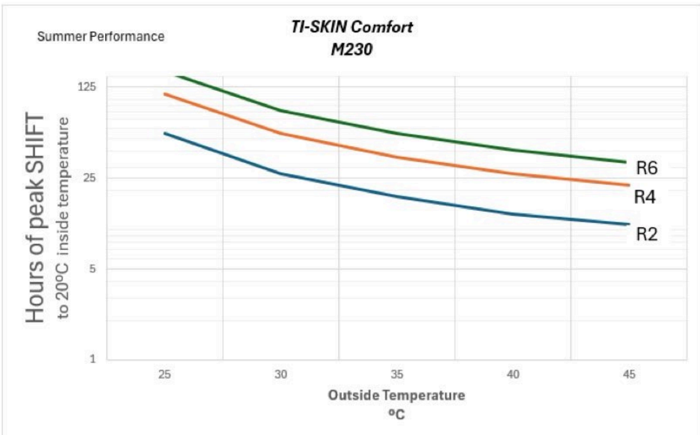

134

Allegato D — pagina 134 del documento originale

Test di laboratorio – Test di flusso termico - R3.3 (R = 3.3 m2.K/W) Verifica con e senza **TI-SKIN**

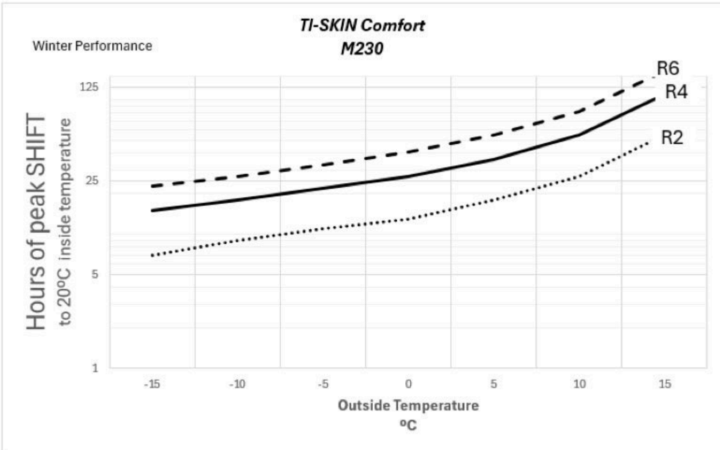

135

Allegato D — pagina 135 del documento originale

Tabella 1 – Confronto prestazioni inverno/estate tra isolanti leggeri e massivi

1 - TEGOLE
2 - INTERCAPEDINE VENTILATA
3 - MEMBRANA TRASPIRANTE
4 - ISOLANTE
5 - FRENO AL VAPORE
6 - PERLINE LEGNO

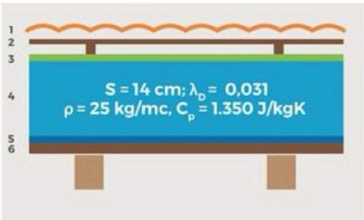

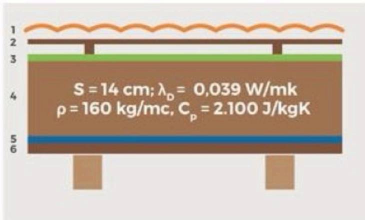

Trasmittanza U [W/mqK]	**0,20**	**0,25**
Trasmittanza periodica Y_{ie} [W/mqK]	**0,178**	**0,103**
Fattore di attenuazione	**0,87**	**0,40**
Sfasamento termico	**3h 10min**	**9h 23min**
Classe prestazione estiva	**V**	**III**
Diffusività termica α[mq/s] isolante	**$0,959 \cdot 10^{-6}$**	**$0,116 \cdot 10^{-6}$**

137

Allegato D — pagina 137 del documento originale

Tabella 2 – Aumenti di spessore dell'isolante massivo per ottenere la stessa U dell'isolante leggero e accoppiamento dell'isolante leggero con PCM per ottenere lo stesso sfasamento termico dell'isolante massivo

1 - TEGOLE 2 - INTERCAPEDINE VENTILATA 3 - MEMBRANA TRASPIRANTE 4 - ISOLANTE 5 - FRENO AL VAPORE 6 - PERLINE LEGNO	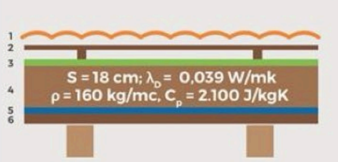 S = 18 cm; λ_D = 0,039 W/mk ρ = 160 kg/mc, C_p = 2.100 J/kgK	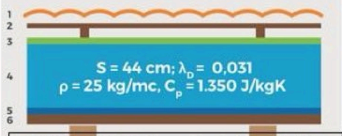 S = 44 cm; λ_D = 0,031 ρ = 25 kg/mc, C_p = 1.350 J/kgK PCM= ρ= 905 kg/mc; C_p=2.496 J/kgK ; λ_D=0,15 (liquid) ; λ_D=0,98 (solid)
Trasmittanza U [W/mqK]	0,20	0,068
Trasmittanza periodica Y_{ie} [W/mqK]	0,05	0,028
Fattore di attenuazione	0,25	0,412
Sfasamento termico	12h 10min	9h 34min
Classe prestazione estiva	I	III
Diffusività termica α[mq/s] isolante	$0{,}116 \cdot 10^{-6}$	$0{,}959 \cdot 10^{-6}$

138

Allegato D — pagina 138 del documento originale

TIPOLOGIE DI APPLICAZIONI RESIDENZIALI – INDUSTRIALI – DIREZIONALI – SANITARIE – ALLEVAMENTI - SERRE

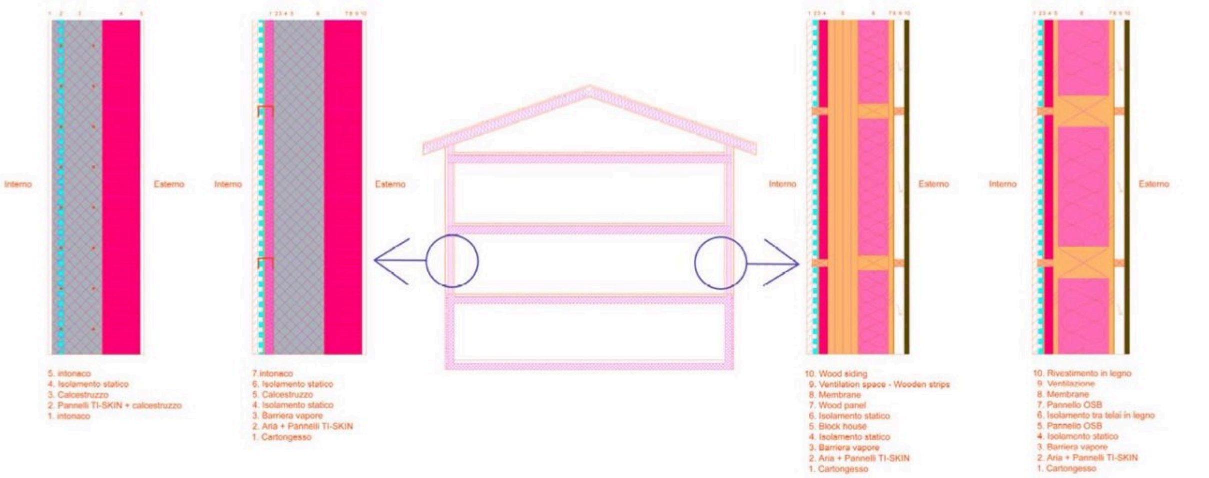

152

Allegato D — pagina 152 del documento originale

TIPOLOGIE DI APPLICAZIONI RESIDENZIALI – INDUSTRIALI – DIREZIONALI – SANITARIE – ALLEVAMENTI - SERRE

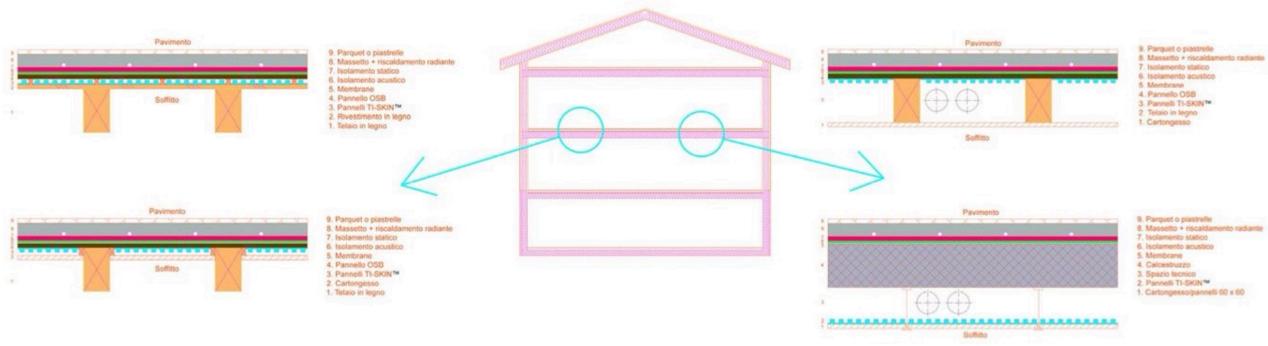

153

Allegato D — pagina 153 del documento originale

TIPOLOGIE DI APPLICAZIONI RESIDENZIALI – INDUSTRIALI – DIREZIONALI – SANITARIE – ALLEVAMENTI - SERRE

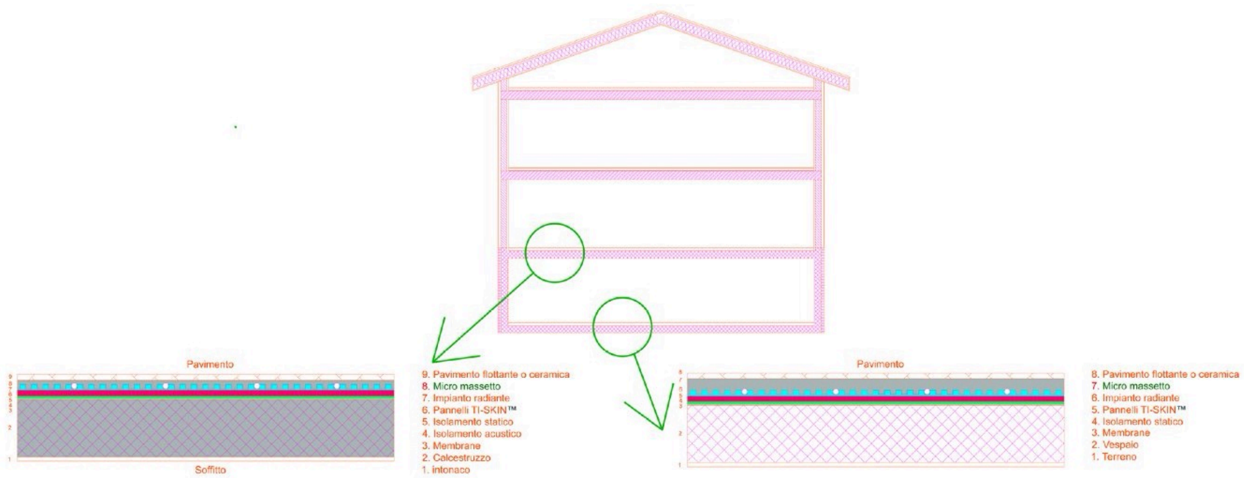

154

Allegato D — pagina 154 del documento originale

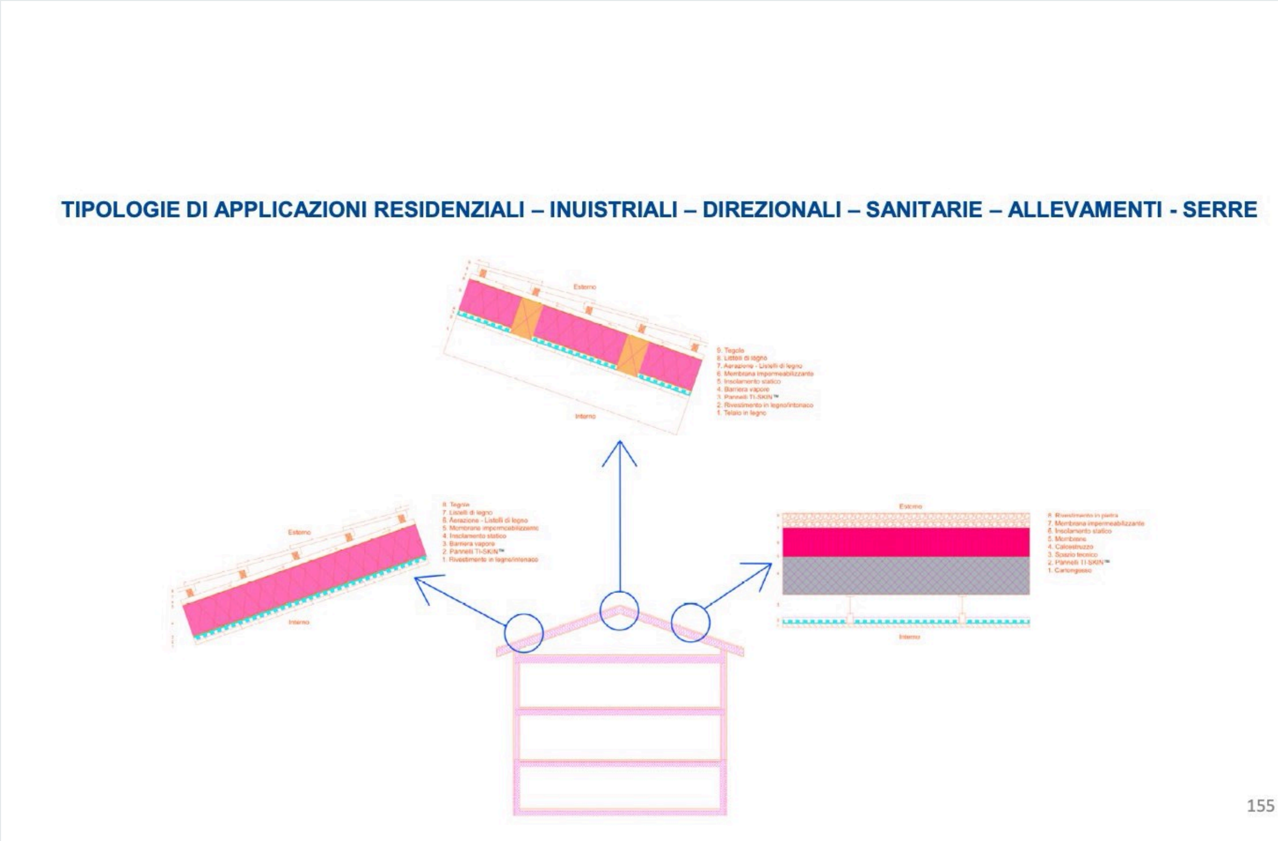

Allegato D — pagina 155 del documento originale